УДК 551.435.4.038:551.14/.15(481:26)

В. ФЬЕЛДСКААР (Исследоват. институт Тектонор Ставангер, Норвегия), А. В. АМАНТОВ (ВСЕГЕИ, Россия)

Перекосы послеледниковых береговых линий побережья Норвегии как свидетельство наличия астеносферы низкой вязкости при слабой изгибной жесткости литосферы*

Скандинавия является одним из ключевых районов исследования ледникового изостатического поднятия. Моделирование поздне- и послеледниковой релаксации Фенноскандии активно развивается в последние годы, но, к сожалению, реологические параметры Земли сильно отличаются у разных исследователей. Большинство специалистов предполагает значительное изменение вязкости от верхней к нижней мантии в сочетании с плотной упругой литосферой.

В результате значительного увеличения вязкости от верхней к нижней мантии компенсирующий изменение нагрузки поток в мантии частично концентрируется в верхней мантии. Такая модель «течения в канале» – одна из возможных крайних гипотез, предложенных более 80 лет назад. Ее противоположная в распределении вязкости альтернатива определяется как модель «глубинного распределенного течения»; она предполагает, что процесс происходит на больших глубинах.

Сопоставление реально наблюдаемых палеоградиентов (перекосов в направлении центральной части Фенноскандии) послеледниковых береговых линий наиболее изученных районов побережья Норвегии с надежными возрастными реперами с моделью с различными параметрами реологии Земли и схемами дегляциации построенных диаграмм береговой линии показывает значительный наклон к центральной части Фенноскандии. Наблюдаемые спектры изменений береговых линий предлагают исключительные перспективы для изучения физических свойств Земли. Модели перекосов древних береговых линий норвежского побережья очень чувствительны к жесткости литосферы и вязкости мантии. Изостатический ответ на дегляциацию Фенноскандии получен с помощью модели Земли с многослойной мантией дифференцированной вязкости под упругой литосферой. Изгибную жесткость последней и вязкость астеносферы изменяли для достижения соответствия между теоретическими и наблюдаемыми перекосами во времени.

Моделирование показало, что наилучшее соответствие с данными наблюдалось при «глубинном распределенном течении» при наличии астеносферы пониженной вязкости (менее чем $7{,}0 \times 10^{19}$ Па с) толщиной менее 150 км, вязкости нижележащей мантии около 10^{21} Па с и эффективной упругой толщине литосферы 30–40 км (что эквивалентно жесткости менее 10^{24} Нм). Модель «течения в канале» при значительном повышении вязкости от верхней к нижней мантии в сочетании с мощной упругой литосферой не может объяснить градиентов наклонов древних береговых линий, наблюдаемых на норвежском побережье.

Ключевые слова: *изостазия, моделирование, реология, голоцен, оледенение, Фенноскандия, Норвегия.*

Willy FJELDSKAAR (Tectonor, Stavanger, Norway), Aleksey AMANTOV (VSEGEI, Russia)

Tilted Norwegian post-glacial shorelines require a low viscosity asthenosphere and a weak lithosphere

Scandinavia is one of the key areas for research on glacial isostatic adjustment. Extensive modeling of the late- and post-glacial rebound in Fennoscandia has been done over the recent years, but unfortunately the suggested Earth rheology varies a lot among the researchers. Most of the researchers argue for a significant viscosity change from upper to lower mantle, combined with a thick elastic lithosphere. We study 5 paleo shoreline gradients with various Earth rheology parameters and various deglaciation models. Shorelines from coastal Norway show significant tilt toward the more central parts of Fennoscandia. The observed shoreline gradients offer exceptional promise for the study of the physical properties of the Earth′s uppermost layers. Our modeling shows that best fit with the observed data is achieved with a 150 km thick lowviscosity asthenosphere with a viscosity of 1.3×10^{19} Pa s above a uniform mantle of viscosity 10^{21} Pa s, and an effective elastic lithosphere thickness (T_e) of 30 km (flexural rigidity ~5×10^{23} Nm). In contrast, models with a significant viscosity increase from upper to lower mantle combined with a thick elastic lithosphere cannot explain the shoreline gradients observed at the Norwegian coast. We suggest that the shoreline gradient information needs to be taken into account in glacial isostatic adjustment modeling.

Keywords: *isostasy, modeling, rheology, Holocene, glaciation, Fennoscandia, Norway.*

Introduction. The Earth has been and still is readjusting after being subjected to huge ice load during the last glaciation. This postglacial rebound in northern Europe enables determination of the underlying Earth rheology, both the effective elastic lithospheric thickness and mantle viscosity. However, there is still debate on the

*Статья публикуется на английском языке.

properties of the lithosphere and whether or not the mantle has a low viscoelastic asthenosphere and a large increase in viscosity to greater depths.

As reviewed in Cathles [4], Daly in 1934 [7] was the first to recognize anomalous uplift behavior in areas peripheral to the former ice sheet. Based on intuition and channel flow models such as those Van Bemmelen and Berlage [25] he expected that mantle material would be squeezed out from under glaciations and produce peripheral bulges. After melting he expected that these peripheral bulges would collapse. However, Daly could not find geological evidence in support of the bulge model. In fact he found that geological data pointed to the opposite behavior of the peripheral areas to what was expected from the bulge hypothesis: late glacial and early post-glacial uplift followed by subsidence.

Daly therefore proposed the "punching" model for explaining how the uplift could give a pattern that was supported by observations. The peripheral areas were dragged down by the lithosphere as the ice-loaded region subsided. When the glacier melted, the central area would drag the peripheral areas above the isostatic equilibrium before they later sank down. Haskell [12] found that the isostatic adjustment of a half-space of uniform viscosity behaved much like Daly's punching model. In a uniform viscosity half-space, flow occurs at great depths. The areas peripheral to the load respond initially sympathetically with the central regions. Unloading would produce an initial regional uplift, before the peripheral areas later would sink back to equilibrium. If the upper mantle is more fluid than the lower mantle, peripheral bulges must be expected upon loading and peripheral troughs upon unloading [5]. Cathles [4] used this kind of discrimination as evidence for an isoviscous 10^{21} Pa s mantle.

These two end member models (channel flow with a thick lithosphere, and deep flow with an asthenosphere and thin lithosphere) are still under debate today, and there is no agreement in the literature on what model that best fits the data of post-glacial rebound. Steffen and Wu [23] give a review of modeling results on Fennoscandian rheology based on observations of post-glacial as well as ongoing uplift in the area. They state that "inversion of RSL (Relative Sea Level) data indicates no low-viscosity zone underneath Scandinavia or that its presence is poorly resolved by the data". However, the BIFROST GPS data (vertical component) favors a thin low-viscosity layer between 160 and 200 km depth [23].

All results on viscosity structure cited in Steffen & Wu [23] use models with significant differences in viscosity between upper and lower mantle (channel flow models). This reflects that the majority of present day modelers relies on the channel flow model. The suggested Earth rheology for Fennoscandia consists of an effective elastic lithosphere thickness (t_e) of 75–160 km, and a viscosity of lower mantle up to 100 times higher than the upper mantle. Earlier studies proposed a lower viscosity asthenosphere on top of the mantle. McConnell (1968) suggested a 200 km thick asthenosphere with 0.1×10^{21} Pa s [16] on top of a mantle of 10^{21} Pa s and increasing with depth, Cathles (1975, 1980) a lithosphere with flexural rigidity 50×10^{23} N m with a 0.04×10^{21} Pa s 75 km thick asthenosphere overlying a uniform 10^{21} Pa s mantle [4, 5], and Wolf (1987) a 100 km thick asthenosphere with 0.012×10^{21} Pa s [26].

Fjeldskaar (1994, 1997) strongly argued for a flexural rigidity of 10^{23}Nm (t_e ~20 km) at the Norwegian coast, increasing to above 10×10^{23} Nm (t_e~50 km) in central parts of Fennoscandia [9, 10]. Fjeldskaar et al. (2000) found that a low viscosity asthenosphere (with thickness less than 150 km thick and viscosity less than 7.0×10^{19} Pa s) over a uniform mantle of viscosity 10^{21} Pa s gives an optimum fit to observed sea level data from Fennoscandia [11].

We have now revisited the Norwegian shoreline diagram data, and modeled the paleo shoreline gradients for various Earth rheology parameters and various deglaciation models, with higher spatial resolution than before. To our knowledge the shoreline diagrams are not used in other recent analyses of the post-glacial rebound. This paper shows, based on analysis of relaxation spectra, rebound in peripheral areas and tilting of paleo shorelines, that the post-glacial rebound in western Norway is best modeled by a deep flow model.

Relaxation spectra. The differences in viscosity structure between deep flow (uniform mantle viscosity) and channel flow models (with a significant viscosity increase from upper to lower mantle) will result in different relaxation time spectra. Relaxation is the time required for an exponentially decreasing variable (as the amplitude of a damped oscillation) to drop from an initial value to 1/e or 0.368 of that value (where e is the base of natural logarithms).

We have selected some recently published Earth models based on the land uplift of Scandinavia (Table 1), and calculated the different relaxation spectra. Except for the model termed "asthenosphere", they are all channel flow models.

The selected examples of channel flow viscosity structure are proposed in recently published studies [2, 20, 13, 22]. Based on deglaciation models ICE-5G [19] and ICE-6G [20] they deduce a preferred Earth rheology under Scandinavia; based on data on the present rate of uplift or relative postglacial sea level data. The viscosity structures vary between the studies, but they all agree that there is a significant increase in the viscosity from upper to lower mantle, i.e. channel flow models. The researchers disagree on the thickness of the elastic lithosphere, but agree that it is relatively thick – between 90 and 160 km (see Table 1 for details). The lithosphere thickness is often termed 'effective elastic thickness', and is related to the stiffness or flexural rigidity of the

Table 1

Various Earth models based on the post-glacial uplift of Scandinavia. Viscosity in astenosphere, upper and lower mantle has unit 10^{21} Pa s

	Lithosphere, km	Asthenosphere	Upper mantle	Lower mantle
Peltier et al. (2015) [20]	90	–	0.5	1.7
Kierulf et al. (2014) [13]	140	–	0.7	2
Steffen et al. (2010) [22]	160	–	0.4	20
Auriac et al. (2016) [2]	120	–	2	50
Asthenosphere [11]	30	0.013	1	1

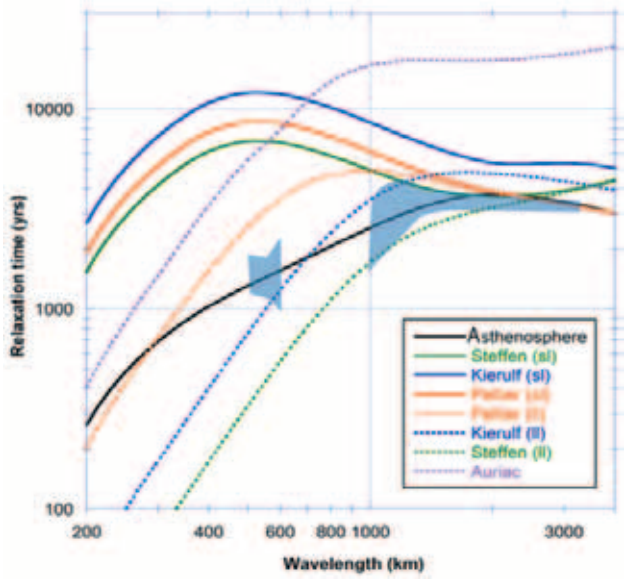

Fig. 1. Relaxation-spectra for the various viscosity models given in Table 1. Curves with solid lines show the relaxation spectra calculated with a thin elastic lithosphere (~30 km), while the dotted lines are for 90–160 km thick elastic lithosphere (according to Table 1). The shaded areas are relaxation spectra (with uncertainties) calculated by McConnell (1968) [16], and inferred by Mitrovica & Peltier [17])

lithosphere. The flexural rigidity describes the resistance to bending under the application of applied, vertical loads.

The relaxation spectra for the various models are shown in Fig. 1. The solid lines show the spectra calculated with a thin elastic lithosphere (~30 km). There are significant differences between the various models. The channel flow model have much higher relaxation time than the "asthenosphere" (deep flow) model at the shorter wavelength load harmonics.

However, as mentioned above the channel flow models also assume a thick elastic lithosphere, between 90 and 160 km thick. Thick elastic lithosphere speeds up the response (reduce the relaxation time). The response reduction is particularly strong for wavelengths lower than 2000 km. The resulting relaxation spectra for the channel flow models are much closer to the "asthenosphere" model when the elastic lithosphere thickness is larger.

McConnell (1968) provided direct evidence of mantle viscosity for Scandinavia [16]. He transformed data of strandlines for central parts of Scandinavia (along a profile from Ångermanland in Sweden to Izhora in Russia) to relaxation spectra of the post-glacial rebound. McConnell's results have been analyzed and updated later [18]. The relaxation spectra [16, 17] are shown by the shaded regions in Fig. 2. These relaxation spectra can be used to evaluate the various viscosity models in Table 1.

As shown in Figure 1 the best match with the relaxation spectra is achieved by the "asthenosphere" model, both for low and high wavelengths. Most of the channel flow models also give a reasonable fit to the observed relaxation spectra. The exception is the preferred model for Fennoscandia of Auriac et al. [2], which has significant deviations from the relaxation spectra (the relaxation spectra for thin lithosphere deviates so strongly that it is not shown in Fig. 1).

The preferred viscosity model of Peltier et al. [20] overestimates the relaxation time by at least 1000 years for low wavelengths. On the other hand, the model of Steffen et al. [22] underestimates the relaxation times for low wavelengths by approximately 400 years. The model of Kierulf et al. [13] overestimates the relaxation time for longer wavelengths.

In summary McConnell's spectra require either a channel flow model with a very thick lithosphere (similar to Daly's down-punching lithosphere), or a deep flow model (similar to Haskell's) with a low-viscosity asthenosphere and a thin lithosphere. The deep flow model gives the best match with McConnell's data, but the cited channel flow models also give reasonable matches with McConnell's data.

Other channel flow models not mentioned here could give better matches. Mitrovica & Peltier [17] found that there is a range of channel flow viscosity models that potentially match McConnell's relaxation spectra – upper mantle viscosities between 3.7 and 4.5×10^{20} Pa s, lower mantle viscosities in the range $1.9–2.2 \times 10^{21}$ Pa and a lithospheric thickness ranging from 70 to 145 km. The bottom line for this discussion is that the relaxation spectra do not have the resolving power to rule out any of the end member viscosity structures and distinguish between channel flow or deep flow models.

However, as mentioned above the two mantle viscosity end members give quite different uplift pattern in peripheral areas, and thick lithosphere strongly reduce shoreline tilts at the ice margins as we discuss below. Let us first compare the Scandinavian peripheral uplift pattern for a deep flow versus channel flow viscosity models and then examine the implications of measured tilts.

Uplift in peripheral areas. Theoretical post-glacial rebound for a channel flow and deep flow model is shown in Fig. 2. As expected, the most significant difference is found in peripheral areas. For the extreme cases the pattern will be this: for the channel flow, peripheral areas will first subside, then uplift. In the deep flow case peripheral areas will first uplift, then subside.

Fig. 2 does not show two extreme cases, but two intermediate cases. But we still see the same phenomena: The deep flow model will give uplift in the peripheral areas, followed by subsidence, while the peripheral areas for the channel flow model will first subside then uplift. Fig. 2 clearly shows that peripheral areas can distinguish deep from channel flow models. This method was used by Cathles [4] to interpret the North American peripheral response noted by Daly to indicate deep mantle flow and an isoviscous adiabatic 10^{21} Pa s mantle. Data could be marshaled in Europe to make the same distinction, but in this paper we focus on using ice margin tilts to constrain lithosphere thickness. We will show that tilting in Scandinavia requires a thin lithosphere and therefore suggests deep flow mantle models are the most appropriate.

Ice Margin Tilts. Observations of the post-glacial shorelines (shoreline diagrams) on the Norwegian coast are perfect for measuring the tilting of past shorelines, and these tilts are for constraining lithosphere thickness, especially when the shorelines are close to the ice margin.

a. Measuring shoreline tilts. The late- and post-glacial sea level in Fennoscandia has been mapped by the following means:

– Shoreline displacement curves, showing the vertical displacement at a certain location,

– Shoreline diagrams, showing the displacement and tilting of paleo shorelines,

– Tide gauge, old water marks, and GPS measurements that record the present relative sea level change.

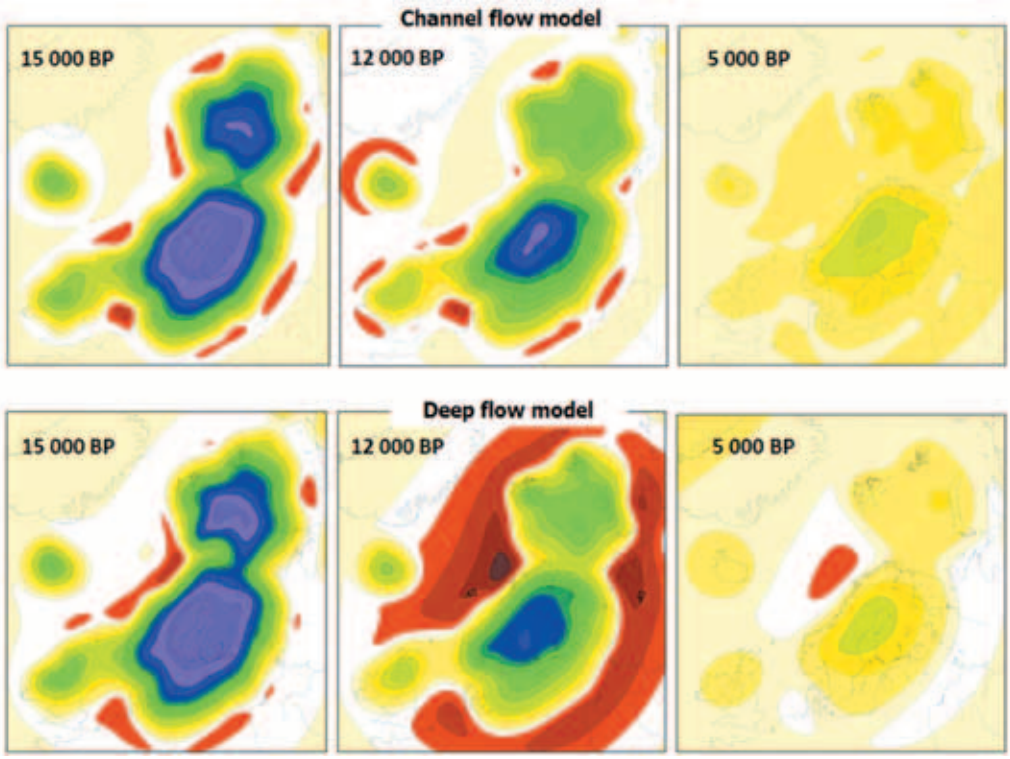

Fig. 2. Calculated uplift at 15 000, 12 000 and 5000 BP for two different Earth rheologies, channel flow vs. deep flow models. Upper figure: channel flow model with a ~100 km thick lithosphere, lower mantle viscosity of 20×10^{22} Pa s and upper mantle viscosity of 0.4×10^{21} Pa s. Lower figures: deep flow model with a ~30 km thick elastic lithosphere above a 75 km low-viscosity asthenosphere (~10^{19} Pa s) and a uniform mantle of viscosity 10^{21} Pa s. The focus of the figure is the uplift pattern of the peripheral areas; the brown color mark areas that have subsided relative to present day (max 50 m). At 5000 BP the channel flow model is still uplifting in the entire region, while the deep flow model is subsiding in the peripheral areas

The advantage of using the tilting of shorelines of some particular age as data to constrain mantle models is that the tilting data is minimally affected by sea level change. The tilting is related essentially only to flow in the mantle and the flexure of the lithosphere.

Five sites along the Norwegian coast with observed shoreline diagrams have been selected for the present investigation; Bergen area (western Norway) [15], Sunnmøre (western Norway) [24], Trøndelag (mid Norway) [14, 24], Lofoten [18] and Finnmark (northern Norway) [21]. Tilting at these sites is determined by shoreline diagrams. A shoreline diagram is a cross-section displaying the elevation and tilt of a shoreline of a particular age. Constructing shoreline diagrams requires the existence of isolation basins at a range of distances from the shoreline that are all near sea level at some particular time in the past. An isolation basin is a basin that can form a lake or be connected to the sea with a small change in land elevation or sea level. To find a number of isolation basins at a range of distances from the shoreline is rare, and there are thus few areas with high quality shoreline diagrams.

Except for location #4 (Lofoten area) the shoreline diagrams are constructed by dating deposits in isolation basins. This is the most precise method available to determine both the elevation and the age of former sea levels.

The method is this: Sediment cores are taken from small lakes and bogs situated at different elevations in a limited area. The position of the former sea level relative to the outlet of these basins determines whether the sediments in the basin are marine, brackish or lacustrine. When sea water flows into the basin the sediments will be marine or brackish. The sediments are then dated, and the date at which each isolation basin became brackish indicates when its outlet was just at sea level. Isolation basins with the same age of brackish transition had the same elevation at the transition, but may now have different elevation if later isostatic uplift was greater inland. This is of course usually the case and so when the elevations of the lakes with the same age brackish transition are plotted as a function of distance from the present shoreline the tilt of the shoreline is indicated. The tilt is often nearly linear. The uncertainty of the tilt depends on the accuracy of the timing of the isolation of each basin, which in turn depends on the number and quality of radiocarbon dates from each basin. Details of the method are provided in [24].

The most precise shoreline diagram is from the Bergen area (#1). This diagram is constructed along a projection plane through eight locations, over a distance of 30–40 km [15]. The gradient of the 12 000 years old shoreline is 1.34 m/km – with a range between 1.25 and 1.44 m/km (Fig. 3). The same method is used to construct shoreline diagrams in locations #2, #3 and #5. The uncertainties are related to the age dating, maximum uncertainty in the age dating is estimated to 5–10 %. The tilts of the Younger Dryas (12 000 BP) shoreline of Bergen (#1) is 1.3 (±0.1) m/km, Sunnmøre (#2) 1.3 (±0.13) m/km, Trøndelag (#3) 1.7 (±0.17) m/km, Lofoten (#4) 1.1 (±0.2) m/km and Finnmark (#5) 0.6 (±0.06) m/km.

The shoreline diagram of location #3 covers an extraordinary long distance (100 km), and the gradient

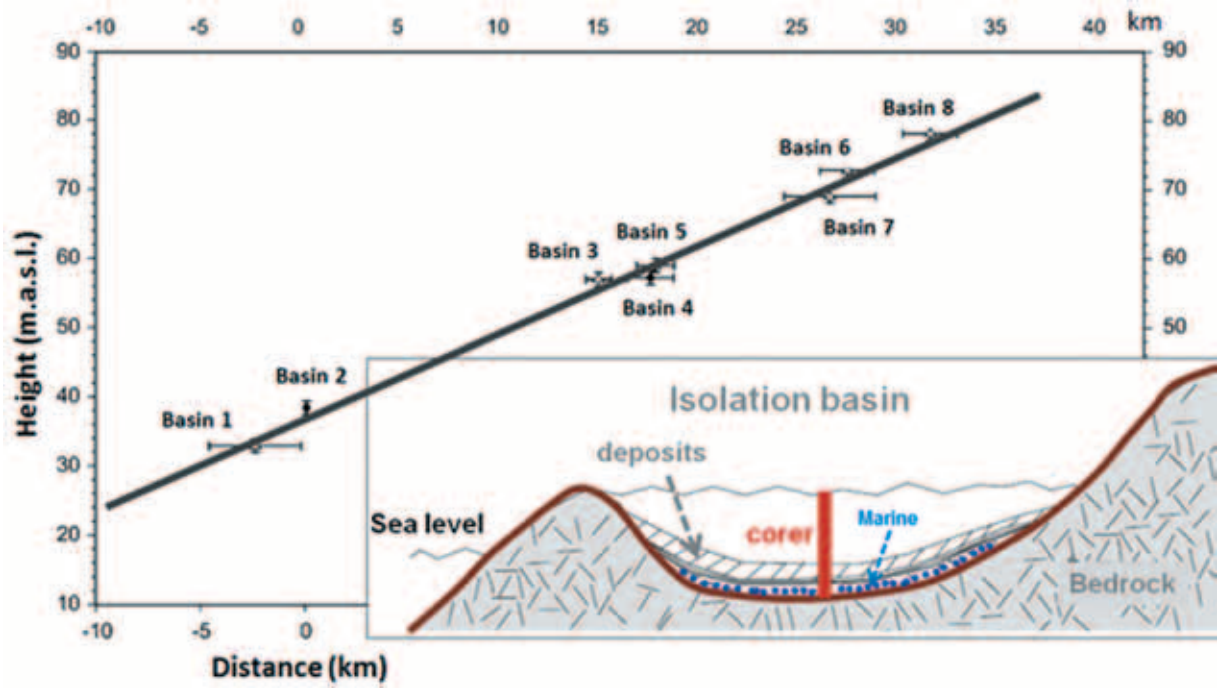

Fig. 3. Shoreline diagram from Bergen area, redrawn from [15]. This diagram uses 12,000 BP sea levels recorded from eight isolation basins over a distance of 40 km. The gradient of the shoreline diagram is 1.3 m/km. Inset sketch shows a cross-section of an isolation basin with lacustrine, brackish and marine deposits. Age dating of the core will give the exact time when sea level fell below the threshold of the lake. The basin would give one point in a shoreline diagram; to construct a full sea level diagram data from several basins at different altitudes are needed

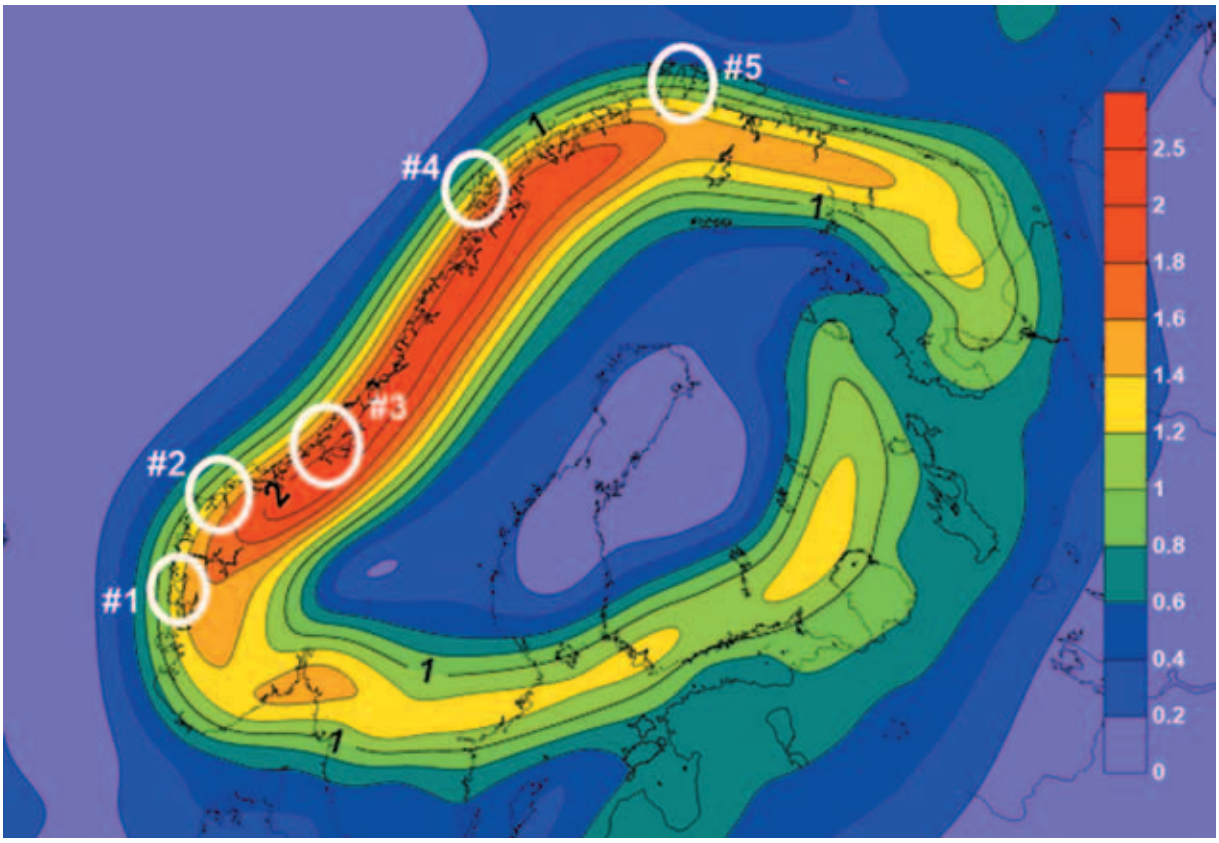

Fig. 4. Locations of the observed paleo shoreline gradients used as calibration for our calculations (white circles). The colors show calculated shoreline gradients at 12 000 BP for Model 1 in Table 2. This model uses deglaciation AA1, has a low viscosity asthenosphere (0.013×10^{21} Pa s), a 10^{21} Pa s mantle, and a lithosphere rigidity 5×10^{23} Nm (elastic thickness ~30 km). The contour interval is 0.2 m/km

in the inner part is higher (>1.7 m/km) than the outer part. All locations are shown in Fig. 4.

b. Calculating shoreline tilts. In principle, three factors could contribute to the tilts of the paleo shorelines:

– Sediment isostasy; the Earth's response to redistribution of rocks,

– Hydro isostasy; the Earth's response to changes in water load,

– Glacial isostasy; the Earth's response to changes in glacial load.

Sediment isostasy. Glacial erosion and sedimentation was modelled by Amantov and Fjeldskaar (2013) over a 1000 year time intervals utilizing a largely automated interpretation of regional geological and geomorphological observations [1]. The modeled redistribution of sediments, however, has no significant impact on the gradients of the paleo shorelines along the Norwegian coast.

Hydro-isostasy depends eustatic (meltwater additions to the ocean) changes, but also on the paleo relief, because the extent of the area covered by water has not been constant through time. The paleo relief is a function of the glacial isostatic response. The area covered with water (ocean or lake) depends on the area covered with glaciers. Fig. 5 (from [1]) shows the spatial distribution of water used in the calculations of hydro-isostasy in combination with eustatic sea level. The eustatic sea level changes over time, according to Fairbanks [8], were applied on the spatial distribution of oceans as shown on Fig. 5. Hydro-isostasy will cause a small inerlase in the tilt of the shorelines because they are all dipping towards the ocean.

Glacial isostasy. The Earth's response to glaciers is here modeling by using a flat Earth layered viscous model overlain by an elastic lithosphere. For more details on the modelling technique, see [9, 10]. It was shown in [10] that calculated isostatic equilibrium deflections by our flat Earth filtering technique show insignificant deviations to the deflections calculated for an isotropically elastic, uniformly thin, spherical shell (presented in [3]) for a load up to 1000 km in radius.

Another potential source of error with our method is that it ignores the coupling between the lithosphere and mantle. To quantify the errors introduced by neglecting full coupling, Fjeldskaar [10] calibrated against analytical solutions for a spherical shell and showed that it agrees within ±10 % with viscoelastic models of the lithosphere [16]. Thus our filtering method introduces some errors, but the errors are scarcely of practical significance for modelling of the postglacial uplift.

The main challenge for a regional flat Earth model is that it cannot provide detailed sea level changes as a global model can. The advantage, however, is that the modelling can be done with high-resolution and short CPU time. The spatial resolution in the modeling reported here is 10 km.

Deglaciation history. We use different deglaciation histories in the modeling: a deglaciation history of our own design (Fig. 6, AA1) and Peltier's ICE-5G [19] and ICE-6G [20] deglaciation histories.

The method used to compute AA1 ice-sheet thickness consists of the following steps (more details are given in [1]):

– Estimation of a general ice-sheet with averaged values and shapes associated with the viscoplastic flow of ice known from present day ice-sheets,

– Modification of ice-thickness distribution and different ice flow velocities due to sub-glacial topography,

– Corrections of ice-thickness by ice-streams, topographic roughness at the ice base, areas of discharge, etc.

The full reconstructed deglaciation history used in the calculations is shown in Fig. 6. Fig. 7 compares the ice thicknesses of AA1 and Peltier's ICE-5G [19] and ICE-6G [20] deglaciation models at 12 000 years BP. This is the time when the studied shoreline gradients were established along the Norwegian coast, and is the main contributor to the shoreline gradients at 12 000 BP. It is worth mentioning that the ice margin in southwestern Norway experienced a major ice-sheet re-advance of at least 40 km in Younger Dryas [15]. There is uncertainty related to the initiation and duration of this re-advance, which may affect the calculated tilting.

Using shoreline tilts to distinguish Earth model. We have found earlier [9–11] that best fit with the observed present rate of uplift and Younger Dryas shoreline tilts was achieved with an effective elastic thickness of less than 30–40 km (flexural rigidity less than 10^{24} Nm), a low-viscosity asthenosphere (viscosity less than 7.0×10^{19} Pa s) above a uniform mantle of viscosity 10^{21} Pa s. With these parameters and using the method described above, the calculated gradients of

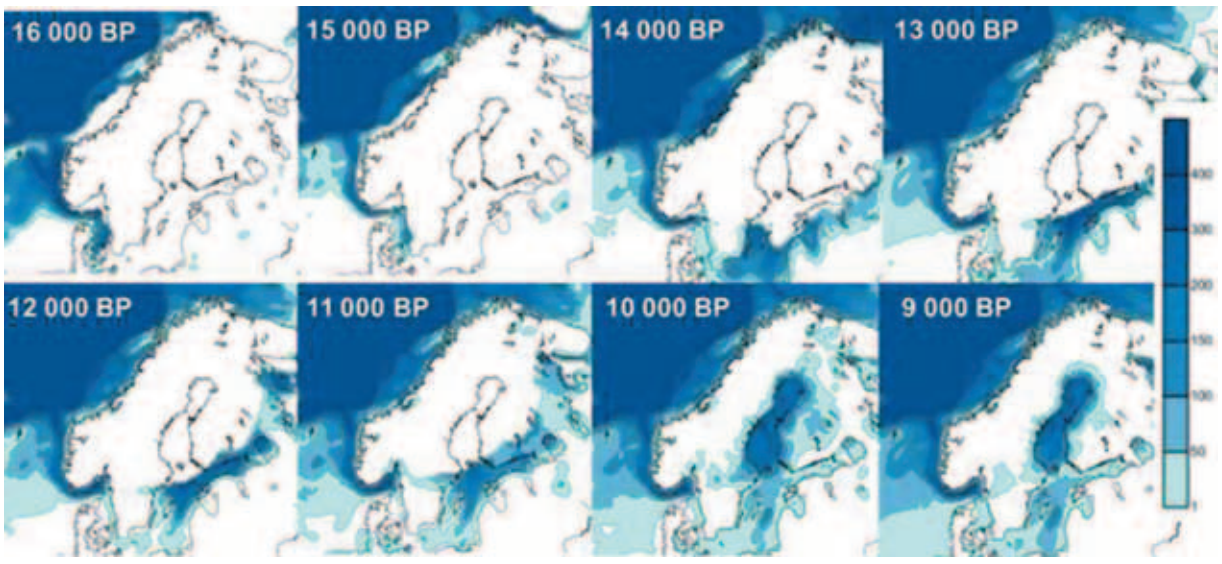

Fig. 5. Estimated post-glacial paleo bathymetry for 1000 years intervals from 16 000 to 9000 BP; Fairbanks (1989) [8] is used as a measure of the eustatic change. From [1]

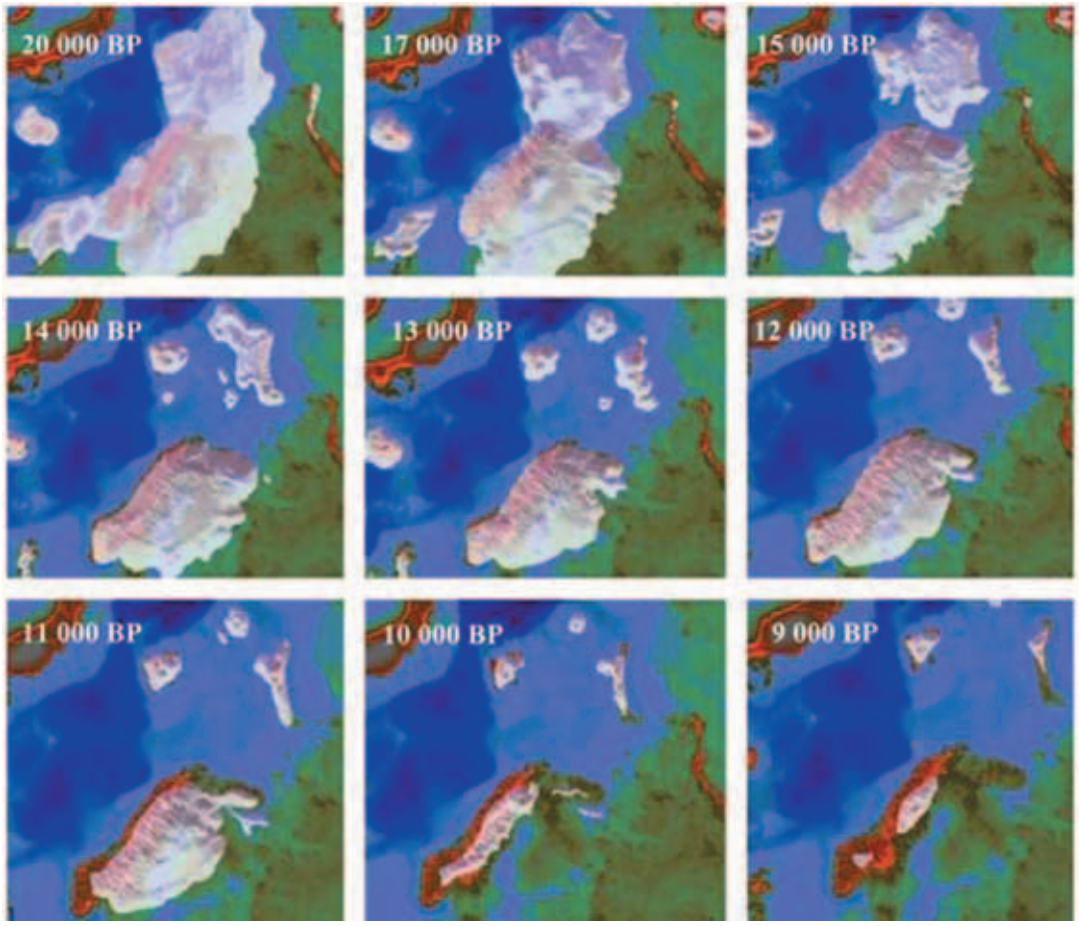

Fig. 6. Deglaciation model AA1 used in the calculations. From [1]

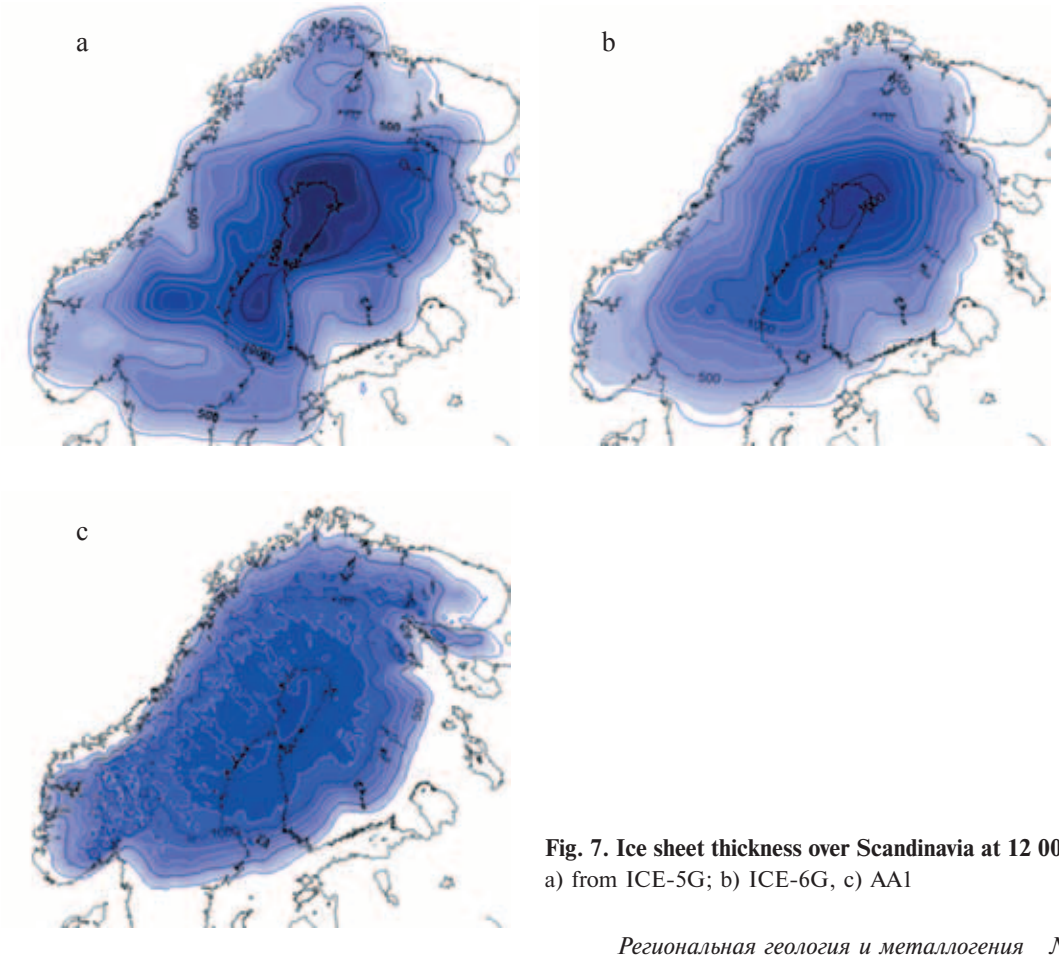

Fig. 7. Ice sheet thickness over Scandinavia at 12 000 BP
a) from ICE-5G; b) ICE-6G, c) AA1

Table 2

Earth models used in the calculations

Model	ICE model	Lower mantle viscosity, Pa s	Upper mantle viscosity, Pa s	Asthenosphere viscosity, Pa s	Lithosphere thickness, km
1	AA1	10^{21}	10^{21}	1.3×10^{19}	30
2	ICE-5G	10^{21}	10^{21}	1.3×10^{19}	30
3	AA1	10^{21}	10^{21}	1.3×10^{19}	90
4	ICE-5G	1.7×10^{21}	0.5×10^{21}	-	100
5	ICE-6G	1.7×10^{21}	0.5×10^{21}	-	30
6	ICE-5G	20×10^{21}	0.4×10^{21}	-	160
7	ICE-5G	2×10^{21}	0.7×10^{21}	-	140

Table 3

Observed and calculated gradients of the 5 Norwegian locations, m/km

Location	**Observed**	Model 1	Model 2	Model 3	Model 4	Model 5	**Model 6**	Model 7
#1	**1.3**	1.3	1.3	0.7	*0.8*	0.7	**0.6**	0.5
#2	**1.3**	1.3	1.2	0.9	0.9	0.8	0.7	0.7
#3	**1.7**	1.8	1.7	1.2	1.2	1.1	0.9	0.9
#4	**1.1**	1.1	1.1	0.9	1.1	1.0	0.8	0.8
#5	**0.6**	0.6	1.2	0.7	0.7	0.7	0.6	0.6

the 12 000 BP shorelines of Fennoscandia are as shown in Fig. 4. This is for Model 1 in Table 2, which give optimum match with the observed gradients for the five locations (Fig. 12, Table 3).

The first question to be clarified is to what extent the match between the tilts calculated by Model 1 and those observed is dependent on the deglaciation model used in the isostatic calculations. We address this question in Model 2 by substituting ICE-5G for deglaciation model AA1. The tilts for Model 2 (Fig. 8) are different from Model 1 (Fig. 4), but still fits the observed shoreline diagrams reasonably well (Table 3 and Fig. 12). Thus, the match between observed and calculated shoreline gradients is not very dependent on the deglaciation model. The fit between observed and calculated tilts is almost as good with ICE-5G as with AA1 (except for the tilt at location #5).

The next question is whether the match with the observations is equally good for other models of Earth rheology, i.e. channel flow models which require a thick lithosphere. Fig. 9 shows that this is not the case. Compared to the case with thin lithosphere (Fig. 4 and 8), the

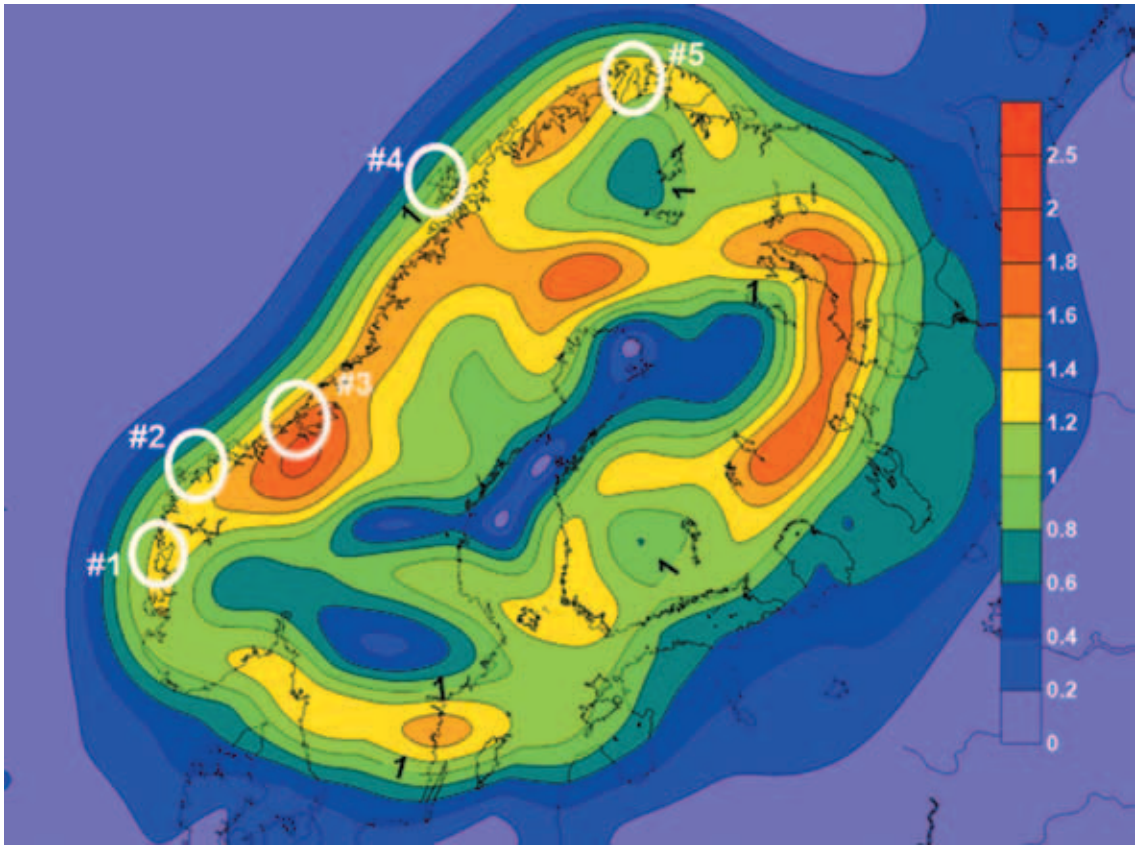

Fig. 8. Calculated shoreline gradients at 12 000 BP (Model 2), modeled with deglaciation model ICE-5G, low viscosity asthenosphere (1.3×10^{19} Pa s) and lithosphere rigidity 5×10^{23} Nm (elastic thickness ~30 km). Contour interval is 0.2 m/km

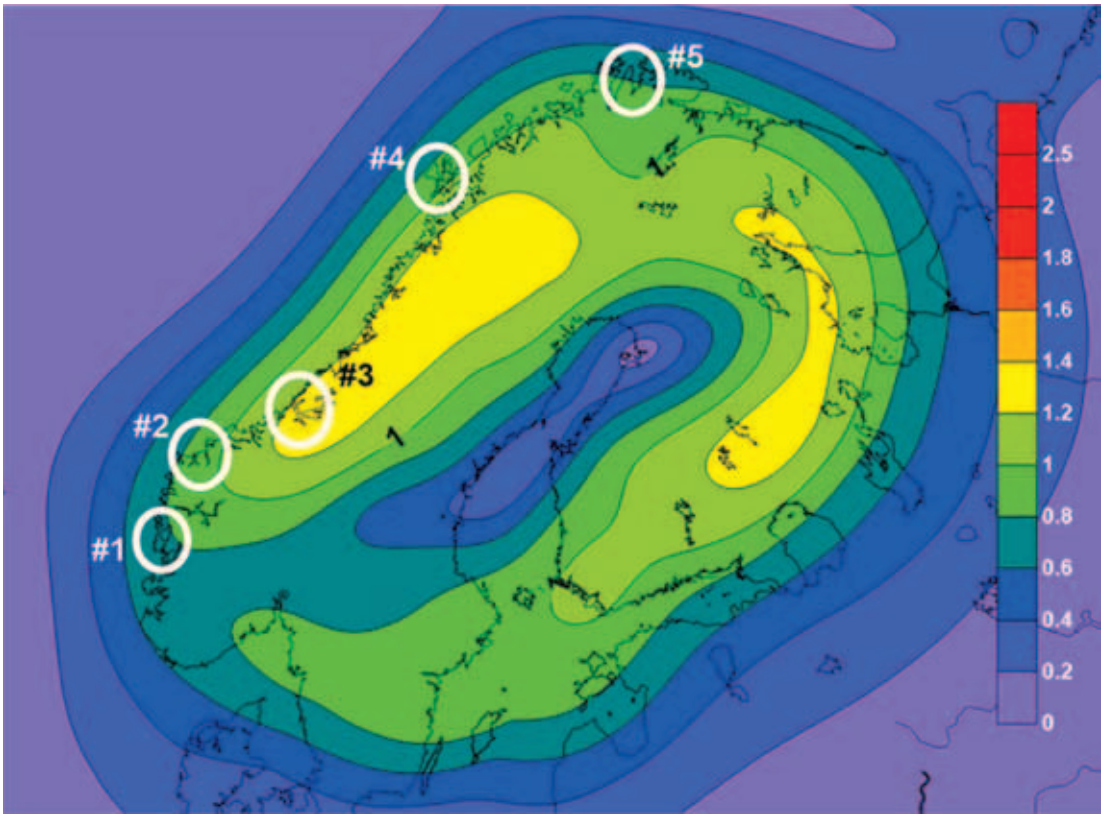

Fig. 9. Calculated shoreline gradients at 12 000 BP for Model 3, with ice history model AA1, low viscosity asthenosphere (1.3×10^{19} Pa s) and lithosphere rigidity 5×10^{24} Nm (elastic lithosphere thickness ~90 km). Contour interval is 0.2 m/km

calculated gradients for elastic lithosphere thickness of ~90 km of Model 3 are reduced almost in half in southwestern Norway (location #1), and also significantly reduced at locations #2 and #3. The mismatch to the observations is shown in Fig. 12 and Table 3. A lithosphere rigidity of 5×10^{24} Nm (elastic lithosphere thickness ~90 km) gives too low gradients. Thus there seems to be an upper bound on the elastic lithosphere based on the paleo shoreline gradients. The upper bound of elastic lithosphere thickness is significantly less than 90 km.

What about the mantle viscosities? Will different viscosity profiles affect the calculated shoreline gradients? Examples of various channel flow models (*Models 4–7)* with the calculated tilts are presented in Fig. 10 and 11.

Fig. 10 shows the gradients with a viscosity model from Peltier [20] and deglaciation models ICE-5G (Model 4) and ICE-6G [19, 20] (Model 5). The upper mantle viscosity is 0.5×10^{21} Pa s, the lower mantle viscosity of 1.7×10^{21} Pa s, and the lithosphere rigidity 5×10^{24} Nm (t_e ~90 km). The mismatch of *Model 5* to the observations is more severe than for *Model 3*, which is a deep flow model with a thick lithosphere. This mantle viscosity profile and deglaciation history makes the tilt agreement worse.

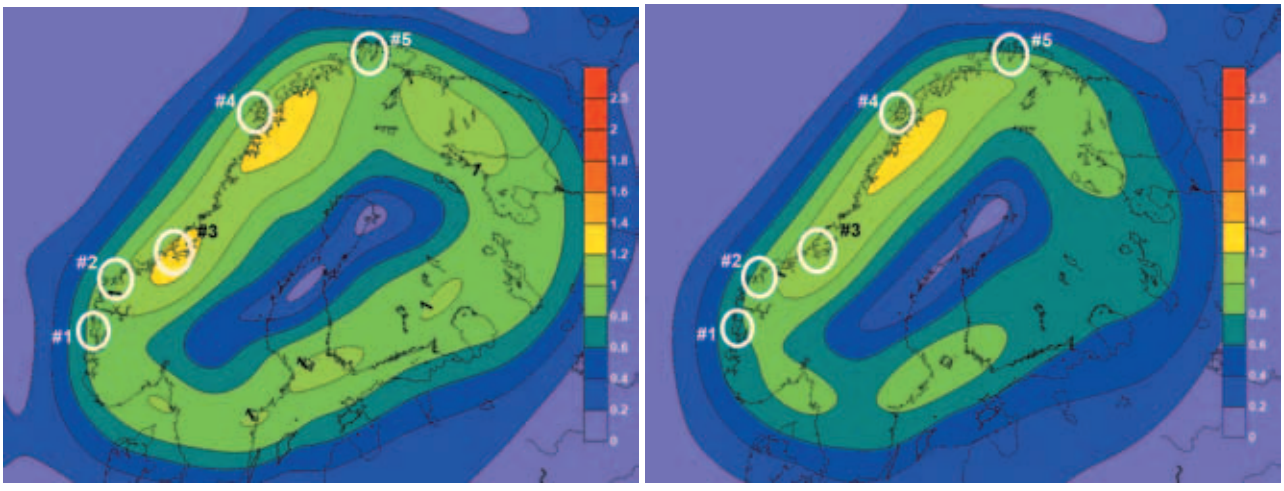

Fig. 10. Calculated shoreline gradients at 12 000 BP; modeled with ICE-5G (Model 4, left) and ICE-6G (Model 5, right), both with upper mantle viscosity 0.5×10^{21} Pa s, lower mantle viscosity 1.7×10^{21} Pa s and lithosphere rigidity 5×10^{24} Nm (te ~90 km). Contour interval is 0.2 m/km

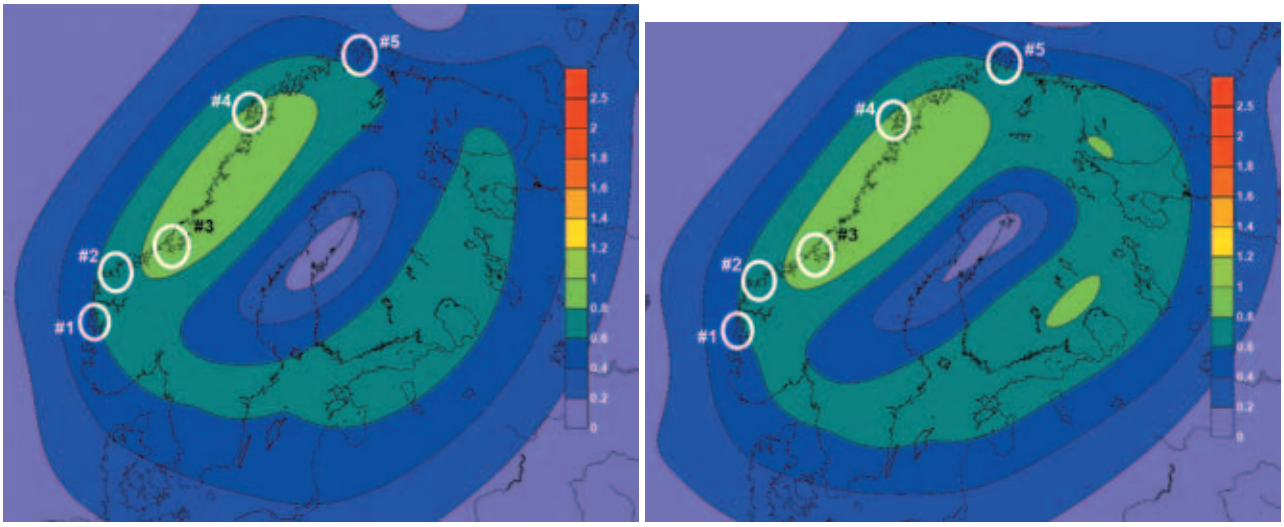

Fig. 11. Calculated shoreline gradients at 12 000 BP for Models 6 and 7, left (Model 6): upper mantle viscosity 0.4 × 10^{21} Pa s, lower mantle viscosity 20 × 10^{21} Pa s and lithosphere rigidity 4 × 10^{25} Nm (te ~160 km); deglaciation model is AA1. Right (Model 7): upper mantle viscosity 0.7 × 10^{21} Pa s, lower mantle viscosity 2 × 10^{21} Pa s and lithosphere rigidity 3 × 12^{25} Nm (te ~140 km). The deglaciation model is ICE-5G. Contour interval is 0.2 m/km

Fig. 11,*a* shows the tilts calculated with the rheology suggested by Steffen et al. [22] with the AA1 deglaciation. The upper mantle viscosity 0.4×10^{21} Pa s, lower mantle viscosity 20×10^{21} Pa s and lithosphere rigidity 4×10^{25} Nm (t_e ~160 km). This Earth rheology (*Model 6*) gives even worse mismatch to the observations compared to *Model 5* (cf. Fig. 12 and Table 3).

Fig. 11,*b* shows the calculated gradients using the preferred viscosity model of Kierulf et al. [13] and the ICE-5G deglaciation (*Model 7*). The upper mantle viscosity is 0.7×10^{21} Pa s, lower mantle viscosity 2×10^{21} Pa s, and a lithosphere rigidity of 3×10^{25} Nm (t_e ~140 km). The mismatch with the observations for this rheology is similar to *Model 6* (Fig. 12 and Table 3).

It is clear from Fig. 12 and Table 3 that best fit with the observed tilts in western Norway at 12 000 BP is achieved with a deep flow model – with an effective elastic thickness of ~30 km (flexural rigidity $\sim5\times10^{23}$ Nm), a low-viscosity asthenosphere of thickness of 75 km and viscosity of 0.013×10^{21} Pa s above an otherwise uniform

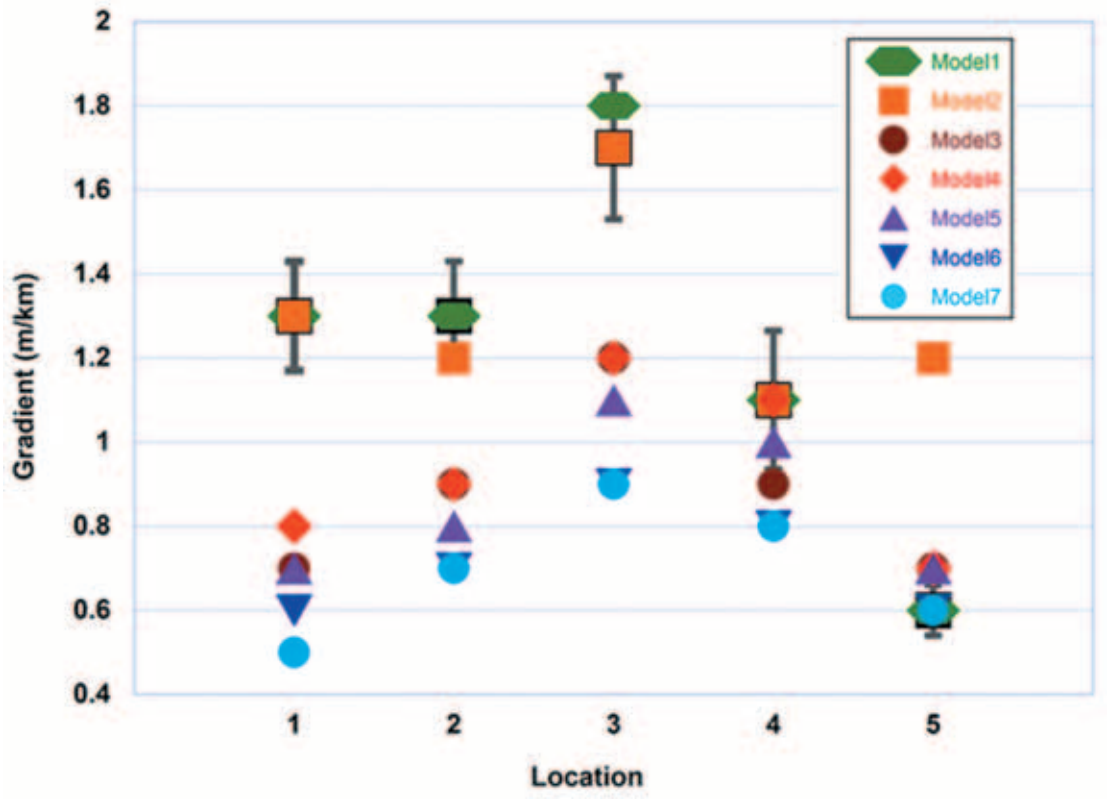

Fig. 12. Observed (black squares with uncertainties) and calculated gradients for the five locations (locations, Fig. 8)

mantle of viscosity 10^{21} Pa s. Channel flow models (exemplified by *Models 4–7*) are not able to explain the observed post-glacial shoreline diagrams in Norway.

Conclusions. Our analysis shows that best fit with the observed tilts of paleoshorelines in Norway is achieved with a deep flow model: a uniform mantle of viscosity 10^{21} Pa s overlain by a low-viscosity 75 km asthenosphere with a viscosity of 0.013×10^{21} Pa s and capped by a thin lithosphere with an effective elastic thickness of ~30 km (flexural rigidity ~5×10^{23} Nm). The ice model is not of great importance for the calculated tilts. The lithosphere thickness is the controlling factor. Channel flow models (exemplified by *Models 4–7*) require thick lithospheres to match McConnell's relaxation spectra, but with these thick lithospheres they are not able to match the observed post-glacial shoreline tilts in Norway.

Shoreline tilts thus seem to be the best way to resolve the channel-flow-thick-lithosphere vs deep-flow conundrum, and they clearly indicate deep flow. This means that the peripheral areas should be subsiding as indicated by the brown ring in the lower panels in Fig. 2, and this prediction could provide a further test of the deep flow models.

We would like to thank Jan Mangerud, Holger Steffen, Stein Bondevik and Lawrence Cathles for constructive comments to an earlier version of this manuscript. Part of this study was sponsored by Academy of Finland and Russian Foundation for Basic Research, RFBR projects 14-05-91763 and 15-05-08169. CISU project funded by Russian Foundation for Basic Research.

1. *Amantov A., Fjeldskaar W.* Geological-geomorphological features of the Baltic region and adjacent areas: imprint on glacial – postglacial development // Regional geology and metallogeny. 2013. № 53. – P. 90–104.

2. *Auriac A., Whitehouse P.L., Bentley M.J.* et al. Glacial isostatic adjustment associated with the Barents Sea ice sheet: A modeling inter-comparison // Quaternary Science Reviews. 2016. Vol. 147. – Pp. 122–135. http://dx.doi.org/10.1016/j.quascirev.2016.02.011.

3. *Brotchie J.F., Silvester R.* On crustal flexure // J. Geophys. Res. 1969. № 74. – P. 5240–5252.

4. *Cathles L.M.* The Viscosity of the Earth's Mantle // Princeton Univ. Press. Princeton, N.J. 1975. – 386 p.

5. *Cathles L.M.* Interpretation of postglacial isostatic adjustment phenomena in terms of mantle rheology / Ed. by N.A. Mörner // Earth Rheology, Isostasy and Eustasy. 1980. – P. 11–45.

6. *Cathles L., Fjeldskaar W.* Comment on "The inference of mantle viscosity from an inversion of the Fennoscandian relaxation spectrum" by J.X. Mitrovica and W.R. Peltier // Geophys. J. Int. 1996. № 127. – P. 489–492.

7. *Daly R.A.* The changing world of the ice age // New Haven: Yale University Press. 1934.

8. *Fairbanks R.G.* A 17,000 year glacio-eustatic sea level record: influence of glacial melting rates on the Younger Dryas event and deep ocean circulation // Nature. 1989. № 342. – P. 637–642.

9. *Fjeldskaar W.* Viscosity and thickness of the asthenosphere detected from the Fennoscandian uplift // Earth and Planetary Science Letters. 1994. № 126. – P. 399–410.

10. *Fjeldskaar W.* The flexural rigidity of Fennoscandia inferred from the post-glacial uplift // Tectonics. 1997. № 16. – P. 596–608.

11. *Fjeldskaar W., Lindholm C., Dehls J.F, Fjeldskaar I.* Post-glacial uplift, neotectonics and seismicity in Fennoscandia // Quaternary Science Reviews. 2000. Vol. 19. – P. 1413–1422.

12. *Haskell N.A.* The motion of a viscous fluid under a surface load // Physic. 1935. № 6. P. 265–269.

13. *Kierulf H.P., Steffen H., Simpson M.J.R.* et al. A GPS velocity field for Fennoscandia and a consistent comparison to glacial isostatic adjustment models // J. Geophys. Res. Solid Earth. 2014. № 119. – P. 6613–6629, doi:10.1002/2013JB010889.

14. *Kjemperud A.* Late Weichselian and Holocene shoreline displacement in the Trondheims-fjord area, central Norway // Boreas. 1986. № 15. – P. 61–82.

15. *Lohne Ø.S., Bondevik S., Mangerud J., Svendsen J.I.* Sea-level fluctuations imply that the Younger Dryas ice-sheet expansion in western Norway commenced during the Allerød // Quaternary Science Reviews. 2007. № 26. – P. 2128–2151.

16. *McConnell R.K.* Viscosity of the mantle from relaxation spectra of isostatic adjustment // J. Geophys. Res. 1968. № 73. – P. 7089–7105.

17. *Mitrovica J.X., Peltier W.R.* The inference of mantle viscosity from an inversion of the Fennoscandian relaxation spectrum // Geophys. J. Int. 1993. № 114. – P. 45–62.

18. *Møller J.J.* Geometric simulation and mapping of Holocene relative sea-level changes in northern Norway // *J. Coast. Res.* № 5. 1989. – P. 403–417.

19. *Peltier W.R.* Global Glacial Isostasy and the Surface of the Ice-Age Earth: The ICE-5G (VM2) Model and GRACE // Ann. Rev. Earth and Planet. Sci. 2004. № 32. – P. 111–149.

20. *Peltier W.R., Argus D.F., Drummond R.* Space geodesy constrains ice age terminal deglaciation: The global ICE-6G_C (VM5a) model // J. Geophys. Res. Solid Earth. 2015. №120. – P. 450–487, doi:10.1002/2014JB011176.

21. *Romundset A., Bondevik S., Bennike O.* Postglacial uplift and relative sea level changes in Finnmark, northern Norway // Quaternary Science Reviews. 2011. №30 (19–20). – P. 2398–2421.

22. *Steffen H., Wu P., Wang H.S.* Determination of the Earth's structure in Fennoscandia from GRACE and implications on the optimal post-processing of GRACE data // Geophys. J. Int. 2010. №182 (3). – P. 1295–1310, doi:10.1111/j.1365–246X.2010.04718.x.

23. *Steffen H., Wu P.* Glacial isostatic adjustment in Fennoscandia – a review of data and modelling // J. Geodyn. 2011. №52 (3–4). – P. 169–204, doi:10.1016/j.jog.2011.03.002.

24. *Svendsen J.I., Mangerud J.* Late Weichselian and Holocene sea-level history for a cross-section of western Norway // Journal of Quaternary Scienc. 1987. №2. – P. 113–132.

25. *Van Bemmelen R.W., Berlage H.P.* Versuch einer mathematischen Behandlung geotektonischer Bewegung unter besonderer Berucksichtegung der Undationstheorie // Beitr. Geophys. 1935. №43. – P. 19–55.

26. *Wolf D.* An upper bound on lithosphere thickness from glacio-isostatic adjustment in Fennoscandia // J. Geophys. 1987. №61. P. 141–149.

1. Amantov, A., Fjeldskaar, W. 2013: Geological-geomorphological features of the Baltic region and adjacent areas: imprint on glacial – postglacial development. *Regional geology and metallogeny, 53.* 90–104. St. Petersburg.

2. Auriac, A., Whitehouse, P.L., Bentley, M.J. et al. 2016: Glacial isostatic adjustment associated with the Barents Sea ice sheet: A modeling inter-comparison. *Quaternary Science Reviews, vol. 147.* 122–135. http://dx.doi.org/10.1016/j.quascirev.2016.02.011.

3. Brotchie, J.F., Silvester, R. 1969: On crustal flexure. *J. Geophys. Res., 74.* 5240–5252.

4. Cathles, L.M. 1975: The Viscosity of the Earth's Mantle. *Princeton Univ. Press.* 386. Princeton, N.J.

5. Cathles, L.M. 1980: Interpretation of postglacial isostatic adjustment phenomena in terms of mantle rheology. *In* Mörner, N.A. (ed.): *Earth Rheology, Isostasy and Eustasy.* 11–45.

6. Cathles, L., Fjeldskaar, W. 1996: Comment on "The inference of mantle viscosity from an inversion of the Fennoscandian relaxation spectrum" by J.X. Mitrovica and W.R. Peltier. *Geophys. J. Int.*, 127. 489–492.

7. Daly, R.A. 1934: The changing world of the ice age. *New Haven: Yale University Press.*

8. Fairbanks, R.G. 1989: A 17,000 year glacio-eustatic sea level record: influence of glacial melting rates on the Younger Dryas event and deep ocean circulation. *Nature*, *342.* 637–642.

9. Fjeldskaar, W. 1994: Viscosity and thickness of the asthenosphere detected from the Fennoscandian uplift. *Earth and Planetary Science Letters*, *126.* 399–410.

10. Fjeldskaar, W. 1997: The flexural rigidity of Fennoscandia inferred from the post-glacial uplift. *Tectonics*, *16.* 596–608.

11. Fjeldskaar, W., Lindholm, C., Dehls, J.F., Fjeldskaar, I. 2000: **Post-glacial uplift, neotectonics and seismicity in Fen**noscandia. *Quaternary Science Reviews, vol. 19*. 1413–1422.

12. Haskell, N.A. 1935: The motion of a viscous fluid under a surface load. *Physics, vol. 6.* 265–269.

13. Kierulf, H.P., Steffen, H., Simpson, M.J.R. et al. 2014: A GPS velocity field for Fennoscandia and a consistent comparison to glacial isostatic adjustment models. *J. Geophys. Res. Solid Earth*, 119. 6613–6629, doi:10.1002/2013JB010889.

14. Kjemperud, A. 1986: Late Weichselian and Holocene shoreline displacement in the Trondheims-fjord area, central Norway. *Boreas*, *15.* 61–82.

15. Lohne, Ø.S., Bondevik, S., Mangerud, J. and Svendsen, J.I. 2007: Sea-level fluctuations imply that the Younger Dryas ice-sheet expansion in western Norway commenced during the Allerød. *Quaternary Science Reviews*, *26.* 2128–2151.

16. McConnell, R.K. 1968: Viscosity of the mantle from relaxation spectra of isostatic adjustment. *J. Geophys. Res.*, *73.* 7089–7105.

17. Mitrovica, J.X., Peltier, W.R. 1993: The inference of mantle viscosity from an inversion of the Fennoscandian relaxation spectrum. *Geophys. J. lnt.*, *114.* 45–62.

18. Møller, J.J. 1989: Geometric simulation and mapping of Holocene relative sea-level changes in northern Norway. *J. Coast. Res.*, *5.* 403–417.

19. Peltier, W.R. 2004: Global Glacial Isostasy and the Surface of the Ice-Age Earth: The ICE-5G (VM2) Model and GRACE. *Ann. Rev. Earth and Planet. Sci.*, *32.* 111–149.

20. Peltier, W.R., Argus, D.F., Drummond, R. 2015: Space geodesy constrains ice age terminal deglaciation: The global ICE-6G_C (VM5a) model. *J. Geophys. Res. Solid Earth*, 120. 450–487, doi:10.1002/2014JB011176.

21. Romundset, A., Bondevik, S., Bennike, O. 2011: Postglacial uplift and relative sea level changes in Finnmark, northern Norway. *Quaternary Science Reviews*, *30 (19–20)*. 2398–2421.

22. Steffen, H., Wu, P., Wang, H.S. 2010: Determination of the Earth's structure in Fennoscandia from GRACE and implications on the optimal post-processing of GRACE data. *Geophys. J. Int.*, *182 (3)*. 1295–1310, doi:10.1111/j.1365–246X.2010.04718.x.

23. Steffen, H., Wu, P. 2011: Glacial isostatic adjustment in Fennoscandia – a review of data and modelling. *J. Geodyn. 52 (3–4)*. 169–204, doi:10.1016/j.jog.2011.03.002.

24. Svendsen, J.I., Mangerud, J. 1987: Late Weichselian and Holocene sea-level history for a cross-section of western Norway. *Journal of Quaternary Science*, *2.* 113–132.

25. *Van Bemmelen, R.W., Berlage, H.P.* 1935: Versuch einer mathematischen Behandlung geotektonischer Bewegung unter besonderer Berucksichtegung der Undationstheorie. *Beitr. Geophys. 43.* 19–55.

26. *Wolf, D.* 1987: An upper bound on lithosphere thickness from glacio-isostatic adjustment in Fennoscandia. *J. Geophys., 61.* 141–149.

Fjeldskaar Willy – Head. Scientist, Tectonor, Norway Tectonor, c/o IPa: P.O. Box 8034, N-406, Stavanger, Norway. <wf@tectonor.com>

Amantov Aleksey – Leading Researcher, A.P. Karpinsky Russian Geological Research Institute (VSEGEI). 74, Sredny Prospect, St. Petersburg, 199106, Russia. <4448470@mail.wplus.net>

Фьелдскаар Вилли – доктор философии, гл. науч. сотрудник, исслед. компания Тектонор (Норвегия). Tectonor, c/o IPark, P.O. Box 8034, N-406, Stavanger, Norway. <wf@tectonor. com>

Амантов Алексей Владиславович –канд. геол.-минер. наук, вед. науч. сотрудник, Всероссийский научно-исследовательский геологический институт им. А.П. Карпинского (ВСЕГЕИ). Средний пр., 74, Санкт-Петербург, 199106, Россия. <4448470@mail.wplus.net>